

1 **Clumped isotopes link older carbon substrates with slower rates of methanogenesis**
2 **in northern lakes**

3
4 Authors: Peter M. J. Douglas^{1,2}, Regina Gonzalez Moguel¹, Katey M. Walter Anthony³,
5 Martin Wik⁴, Patrick M. Crill⁴, Katherine S. Dawson^{2,5}, Derek A. Smith^{2,6}, Ella Yanay²,
6 Max K. Lloyd^{2,7}, Daniel A. Stolper⁷, John M. Eiler², Alex L. Sessions²

7
8 1- Department of Earth and Planetary Sciences, McGill University, Montreal, QC,
9 Canada

10 2- Division of Geological and Planetary Sciences, California Institute of Technology,
11 Pasadena, CA, USA

12 3- International Arctic Research Center, University of Alaska-Fairbanks, Fairbanks, AK,
13 USA

14 4- Department of Geological Sciences and Bolin Center for Climate Research, Stockholm
15 University, Stockholm, Sweden

16 5- Department of Environmental Sciences, Rutgers University, New Brunswick, NJ, USA

17 6- Department of Biology, Case Western Reserve University, Cleveland, OH, USA

18 7- Department of Earth and Planetary Sciences, University of California-Berkeley,
19 Berkeley, CA, USA

20
21 **Supplementary Materials**

22 **Supplementary Text and Figures:**

23 *ST1- Details on culture experiment sterile media:*

24 The sterile media used in the pure and enrichment culture experiments contained (g/L):

25 NaCl (23.4), MgSO₄•7 H₂O (9.44), NaHCO₃ (5.0), KCl (0.8), NH₄Cl (1.0), Na₂HPO₄

26 (0.6), CaCl₂•2 H₂O (0.14), cysteine-HCl (0.25), with the addition of 10 mL DSM 141

27 Trace Element solution, 10 mL of DSM 141 Vitamin solution, and 2.5 mL of a 50 mM

28 H₂S⁻ solution.

29 *ST2- Details on $\Delta^{13}\text{CH}_3\text{D}$ and $\Delta^{12}\text{CH}_2\text{D}_2$ Measurements*

30 CH₄ samples from the Batch 3 culture experiments were measured for δD , $\delta^{13}\text{C}$,

31 $\Delta^{13}\text{CH}_3\text{D}$, and for three samples additionally $\Delta^{12}\text{CH}_2\text{D}_2$. For these measurements the

32 relevant equations are:

33
$$\Delta^{13}\text{CH}_3\text{D} = \left(\frac{^{13}\text{CH}_3\text{D}}{^{13}\text{CH}_3\text{D}_R} / \frac{^{13}\text{CH}_3\text{D}}{^{13}\text{CH}_3\text{D}_R^*} - 1 \right) \quad (6)$$

34 $\Delta^{12}\text{CH}_2\text{D}_2 = ({}^{12}\text{CH}_2\text{D}_2\text{R} / {}^{12}\text{CH}_2\text{D}_2\text{R}^* - 1)$ (7)

35 Where the measured and expected random isotope ratios are defined as:

36 ${}^{13}\text{CH}_3\text{D}\text{R} = ([{}^{13}\text{CH}_3\text{D}] / [{}^{12}\text{CH}_4])$ (8)

37 ${}^{12}\text{CH}_2\text{D}_2\text{R} = ([{}^{12}\text{CH}_2\text{D}_2] / [{}^{12}\text{CH}_4])$ (9)

38 ${}^{13}\text{CH}_3\text{D}\text{R}^* = (4 \times {}^2\text{R} \times {}^{13}\text{R})$ (10)

39 and

40 ${}^{12}\text{CH}_2\text{D}_2\text{R}^* = (6 \times [{}^2\text{R}]^2)$ (11)

41 A complete description of the analytical methods used for this measurement is found in
 42 *Eldridge et al.* [2019]. Samples were measured against a working reference gas with
 43 calibrated $\Delta^{13}\text{CH}_3\text{D}$ and $\Delta^{12}\text{CH}_2\text{D}_2$ values of 2.59 ± 0.14 ‰ and 5.86 ± 0.60 ‰,
 44 respectively *Eldridge et al.* [2019]. External reproducibility of δD , $\delta^{13}\text{C}$, $\Delta^{13}\text{CH}_3\text{D}$, and
 45 $\Delta^{12}\text{CH}_2\text{D}_2$ measurements, as determined from repeated measurements of laboratory
 46 standards, was 0.17, 0.02, 0.38 and 1.52 ‰ (1σ standard deviations; n=16), respectively.
 47 *ST3- Rationale for assumptions in model of kinetic isotope effects and comparison to*
 48 *data*

49 We make three assumptions to model the relationship between CH_4 production
 50 rate and Δ_{18} or $\Delta^{13}\text{CH}_3\text{D}$ values, and to compare these model results to empirical data
 51 from culture experiments. First, we assume a constant rate of reverse methanogenesis
 52 (r_{rev}). This implies that reverse methanogenesis is a zero-order reaction. There are few
 53 constraints on the rate of reverse methanogenesis and its variability. However, anaerobic
 54 oxidation of methane (AOM) is thought to proceed using a reverse methanogenesis
 55 pathway [*Timmers et al.*, 2017], and previous studies have inferred zero-order kinetics for

56 AOM at high CH₄ concentrations [Vavilin, 2013; Vavilin and Rytov, 2013], which would
57 be applicable to our culture experiments.

58 Second, to compare empirical results from culture experiments and model
59 predictions, we express r_{rev} and r_{net} normalized to culture media volume. This comparison
60 requires an assumption of uniform cell density between the culture experiments. This
61 assumption is an oversimplification and could be responsible for some of the scatter in
62 our data-model comparison (See ST-5). Accounting for cell density would be valuable in
63 future studies relating Δ_{18} and CH₄ production rates.

64 Third, the model was developed for hydrogenotrophic methanogenesis [Stolper *et*
65 *al.*, 2015], but we are comparing it to CH₄ produced using four different carbon
66 substrates (Figure 1). However, the model specifically describes kinetic isotope effects
67 associated with the addition of a hydrogen atom to methyl-coenzyme-M. This step is
68 common to all of the CH₄ production pathways studied here, and therefore kinetic isotope
69 effects for clumped isotopologues can be reasonably assumed to be similar for these
70 different methanogenesis pathways, as discussed by Gruen *et al.* [2018].

71 To compare the range of CH₄ production rates from thermokarst lake incubation
72 experiments [Heslop *et al.*, 2015] with the modeled relationship between Δ_{18} and r_{net} , we
73 took the full range of reported CH₄ production potentials (0.02 to 8.08 $\mu\text{g C-CH}_4 \text{ g dry}$
74 $\text{sediment}^{-1} \text{ day}^{-1}$) and converted this to $\text{mg CH}_4 \text{ ml pore water}^{-1} \text{ hour}^{-1}$ using mean values
75 of the gravimetric water content for the two sample types (organic rich mud and thawed
76 permafrost) with the highest and lowest CH₄ production rates.

77

78

79 *ST-4 Details on enrichment culture experiment results*

80 The enrichment culture experiments are clearly differentiated from the pure culture
81 experiments in Figure 1. With this limited dataset we cannot clearly identify the cause of
82 this difference. One possibility is a higher rate of the reverse reactions of
83 methanogenesis. If r_{rev} is increased by a factor of 10 (to $5 \times 10^{-3} \text{ mg CH}_4 \text{ hr}^{-1} \text{ ml}^{-1}$) the
84 kinetic isotope effect model provides a relatively good fit to these data (Supplementary
85 Figure 1). This is plausible given that with the diverse consortium of microbes potentially
86 present in these experiments there would have been the possibility of sulfate reduction or
87 other bacterial metabolisms acting as an electron acceptor for AOM, which could have
88 increased the rates of reverse methanogenesis and increased Δ_{18} values [Ash *et al.*, 2019].
89 We note that sulfate was present in the culture media, and there was anecdotal evidence
90 (i.e. odor) of the presence of hydrogen sulfide during gas sampling of these cultures.

91 Alternately, if the methanogen cell density in these experiments was substantially
92 higher than in the pure culture experiments, it is possible that the relatively high net CH_4
93 production rate is not an accurate reflection of the cell-specific CH_4 production rate
94 relative to the pure cultures. However, it is unlikely that the enrichment culture
95 methanogen community would have reached the large turbid densities of the pure culture
96 experiments.

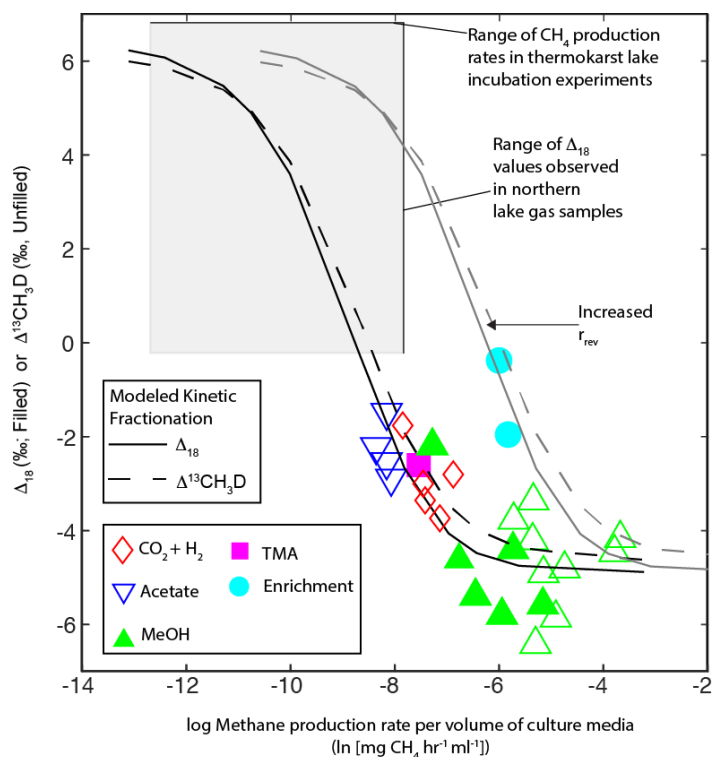
97

98

99

100

101



102

103 **Supplementary Figure 1:** Plot of log CH₄ production rate vs. Δ₁₈ and Δ¹³CH₃D in a
 104 subset of pure and enrichment culture experiments. Solid and dashed lines indicate
 105 predicted values based on a model of methanogenesis kinetic isotope effects [Stolper *et*
 106 *al.*, 2015], assuming a constant value of r_{rev} of 4×10^{-4} mg CH₄ hr⁻¹ ml⁻¹. Gray solid and
 107 dashed lines indicate predicted values with an r_{rev} value of 5×10^{-3} mg CH₄ hr⁻¹ ml⁻¹. Gray
 108 box as in Figure 1. Analytical errors for Δ₁₈ or Δ¹³CH₃D measurements (1σ) are smaller
 109 than the symbols. MeOH, methanol; TMA, Trimethylamine.

110

111

112 *ST-5 Clumped isotope variability in pure culture experiment results and model sensitivity*

113 *to fractionation factors*

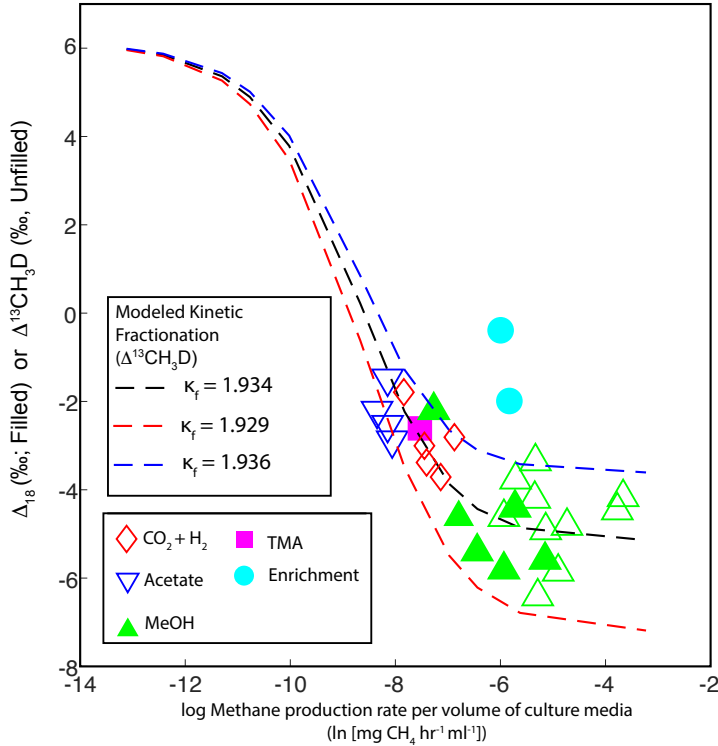
114 The model of kinetic isotope effects predicts the general trend of the pure culture results
 115 shown in Figure 1, but there is clearly variability in these results that is not accounted for
 116 by the model. It is beyond the scope of this study to thoroughly assess the causes of this
 117 variability. However, we observe that varying the value of $\kappa_f^{13}\text{CH}_3\text{D}$ (as defined in the
 118 Methods) from 1.929 to 1.936 generates model curves that encompass the variability in
 119 the pure culture data (Supplementary Figure 2). It is important to note that differences in

120 κ_f - $^{13}\text{CH}_3\text{D}$ would have a much smaller effect at the lower rates of methanogenesis that are
121 generally found in natural environments.

122 The largest differences from the model predicted values occur in the Batch 3
123 experiments (Table 2). These experiments were all conducted using methanol as a
124 substrate, suggesting that differences between methanogenesis pathways are not
125 producing the observed variability. Additionally, these experiments were conducted in
126 smaller batch experiments with less overall substrate provided, and the observed
127 variability may be partly caused by closed-system Rayleigh fractionation effects that
128 would potentially be more pronounced in smaller batch experiments. We observe
129 substantial enrichment of the $\delta^{13}\text{C}$ and δD of CH_4 in our experiments (Supplementary
130 Table 2) that would be consistent with substrate depletion during closed-system Rayleigh
131 fractionation [*Whiticar*, 1999; *Hayes*, 2001].

132 Three measurements of the Batch 3 samples included both $\Delta^{13}\text{CH}_3\text{D}$ and
133 $\Delta^{12}\text{CH}_2\text{D}_2$ values, and therefore afford an opportunity to examine whether the model
134 predictions are consistent with measurements of two distinct clumped isotopologues.
135 These measurements are consistent with the modeled relationship between r_{net} and
136 $\Delta^{12}\text{CH}_2\text{D}_2$ across a relatively narrow range of κ_f - $^{12}\text{CH}_2\text{D}_2$ values (1.62 to 1.64)
137 (Supplementary Figure 3A). Likewise, the measurements are consistent with the model
138 predicted relationship between $\Delta^{13}\text{CH}_3\text{D}$ and $\Delta^{12}\text{CH}_2\text{D}_2$, applying the same range of κ_f -
139 $^{13}\text{CH}_3\text{D}$ as applied in Supplementary Figure 2 (Supplementary Figure 3B). Currently
140 there are few available measurements of $\Delta^{12}\text{CH}_2\text{D}_2$ in the literature, but as this
141 measurement becomes more widespread it will provide additional constraints that can be

142 used to test hypothesized relationships between clumped isotope values and rates of
143 methanogenesis.

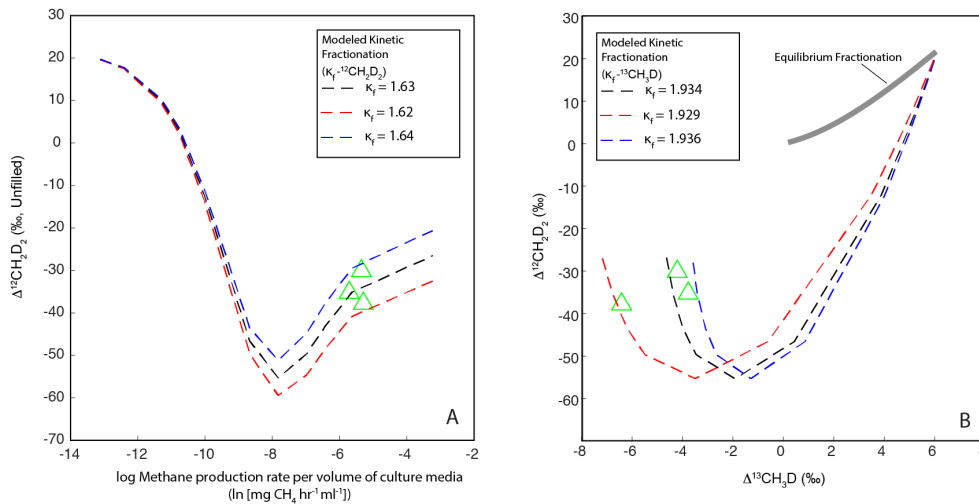


144

145 **Supplementary Figure 2:** Plot of log CH_4 production rate vs. Δ_{18} and $\Delta^{13}\text{CH}_3\text{D}$ in a
146 subset of pure and enrichment culture experiments. Dashed lines indicate predicted
147 values based on a model of methanogenesis kinetic isotope effects [Stolper *et al.*, 2015],
148 with varying values of $\kappa_f^{13}\text{CH}_3\text{D}$ (see Methods), assuming a constant value of r_{rev} of
149 $4 \times 10^{-4} \text{ mg CH}_4 \text{ hr}^{-1} \text{ ml}^{-1}$. Analytical errors for Δ_{18} or $\Delta^{13}\text{CH}_3\text{D}$ measurements (1σ) are
150 smaller than the symbols. MeOH, methanol; TMA, Trimethylamine.

151

152



153

154 **Supplementary Figure 3:** $\Delta^{12}\text{CH}_2\text{D}_2$ results from the Batch 3 pure culture experiments
 155 plotted against (A) the natural log of CH_4 production rate and (B) $\Delta^{13}\text{CH}_3\text{D}$. Dashed lines
 156 indicate predicted values based on a model of methanogenesis kinetic isotope effects
 157 [Stolper et al., 2015], with varying values of $\kappa_f^{12}\text{CH}_2\text{D}_2$ (A) and $\kappa_f^{13}\text{CH}_3\text{D}$ (B), assuming a
 158 constant value of r_{rev} of $4 \times 10^{-4} \text{ mg CH}_4 \text{ hr}^{-1} \text{ ml}^{-1}$. Analytical errors for $\Delta^{12}\text{CH}_2\text{D}_2$ and
 159 $\Delta^{13}\text{CH}_3\text{D}$ measurements (1σ) are smaller than the symbols. Gray line in (B) indicates the
 160 predicted values for equilibrium fractionation [Young et al., 2017].
 161

162 ST-6: Comparison of CH_4 concentration and stable carbon and hydrogen isotopic
 163 composition with Fm values

164 In both lake types we do not observe a significant correlation ($p < 0.05$) between
 165 CH_4 concentration or $\delta^{13}\text{C}$ values and CH_4 Fm values (Supplementary Figure 4). For the
 166 Alaskan dataset there are also measurements of CO_2 $\delta^{13}\text{C}$, and we do not observe a
 167 significant correlation between $^{13}\alpha_{\text{CO}_2\text{-CH}_4}$ and Fm values. We do observe a significant
 168 negative correlation between CH_4 δD and Fm in the Stordalen dataset, although this
 169 correlation is weaker than that between Δ_{18} and Fm. We do not observe a similar
 170 correlation in the Alaskan dataset.

171 In general, a greater proportion of CH_4 derived from acetoclastic
 172 methanogenesis is associated with higher $\delta^{13}\text{C}$ values and lower δD values [Whiticar,

173 1999]. In the Alaskan dataset we do not observe a clear correlation between Fm and these
174 variables. In the Stordalen dataset we observe correlations that are consistent with higher
175 Fm with more acetoclastic methanogenesis. However, culture experiments do not show a
176 significant difference between these pathways for Δ_{18} if CH_4 is produced at the same rate
177 (Figure 1). Furthermore, neither δD nor $\delta^{13}\text{C}$ is as strong a predictor of Fm as is Δ_{18} .
178 Given the inconsistent and relatively weak correlations between δD or $\delta^{13}\text{C}$ and Fm, we
179 conclude that rates of methanogenesis, as opposed to methanogenic pathway, is a more
180 important variable for understanding variability in Fm in these lakes.

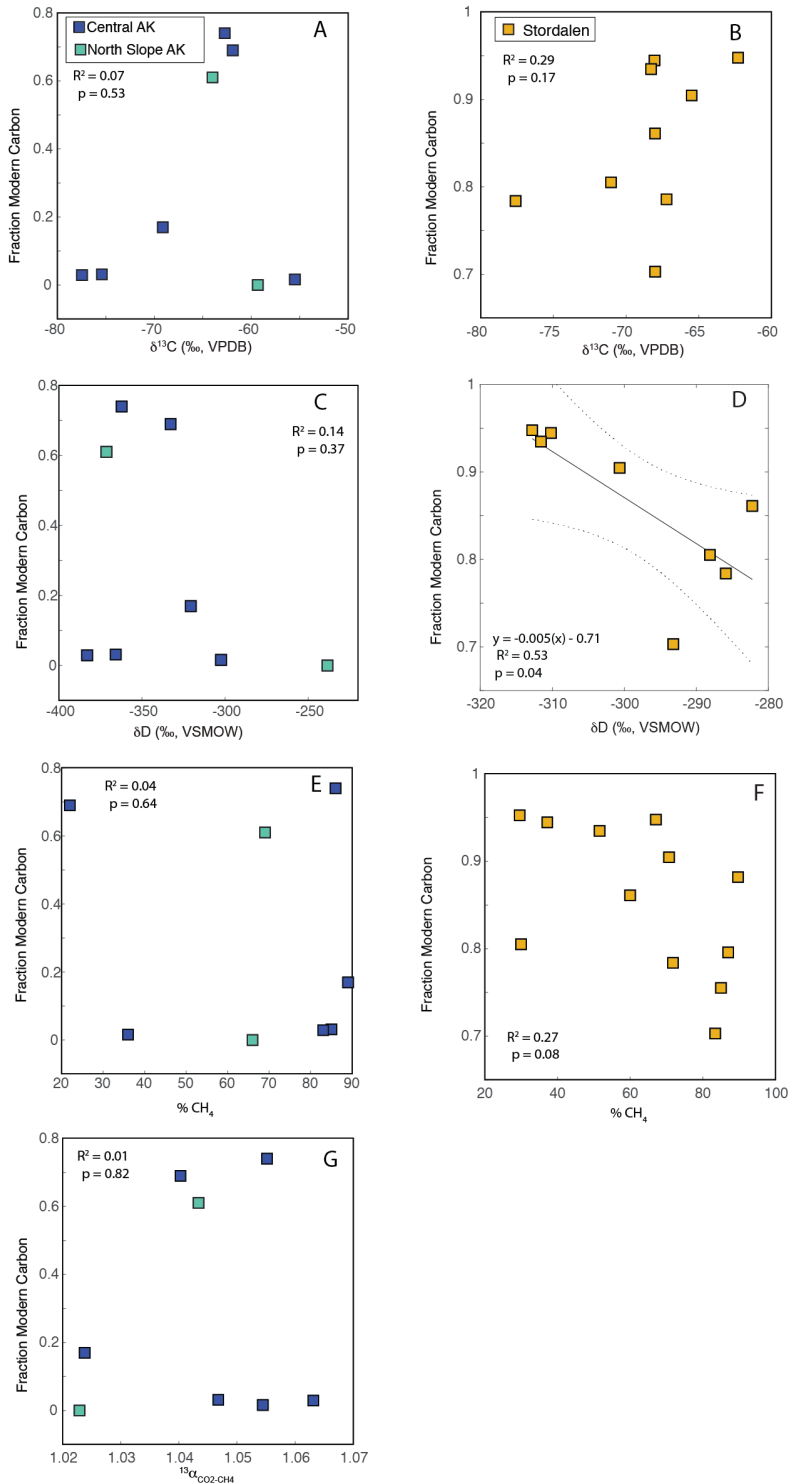
181 Some studies have inferred that variable degrees of anaerobic or aerobic oxidation
182 can influence Δ_{18} values [*Wang et al.*, 2016; *Young et al.*, 2017; *Giunta et al.*, 2019],
183 although the direction of this effect is different for aerobic or anaerobic oxidation, with
184 predicted lower values for aerobic oxidation and higher values for anaerobic oxidation.
185 Greater CH_4 oxidation will generally lead to higher δD and $\delta^{13}\text{C}$ values in CH_4 , and
186 smaller values of $^{13}\alpha_{\text{CO}_2\text{-CH}_4}$ [*Whiticar*, 1999]. We do not observe a pattern that is
187 consistent with oxidation being linked to Fm in either lake type. As discussed above, at
188 Stordalen higher Fm is correlated with higher $\delta^{13}\text{C}$ but with lower δD values, which is
189 not consistent with an oxidation effect. In Alaska there is no apparent correlation between
190 Fm and $\delta^{13}\text{C}$ or $^{13}\alpha_{\text{CO}_2\text{-CH}_4}$.

191 Substrate depletion in a closed system is expected to lead to enrichment of $\delta^{13}\text{C}$ in
192 CH_4 [*Whiticar et al.*, 1999]. Currently the effects of substrate depletion on Δ_{18} have not
193 been explicitly studied. We suggest that the absence of a significant correlation between
194 CH_4 $\delta^{13}\text{C}$ and Fm in either lake system means that this process is not strongly influencing
195 the correlation between Δ_{18} and Fm. As discussed above (ST-5), closed-system substrate

196 depletion may have influenced our pure culture results, but any substrate depletion effects
197 appear to be secondary to the effect of net CH₄ production rate (Supplementary Figure 2).

198

199



200

201 **Supplementary Figure 4:** Scatter plots of CH_4 ^{14}C age vs. different isotopic or chemical
 202 parameters for the Alaskan and Stordalen datasets. (A) and (B): $\delta^{13}\text{C}$ of CH_4 ; (C) and (D)
 203 δD of CH_4 ; (E) and (F) CH_4 concentration (% by volume); (G) $^{13}\alpha_{\text{CO}_2\text{-CH}_4}$ (Alaskan dataset
 204 only). R^2 and p values are shown for each correlation. In (D) the solid line shows the
 205 best-fit regression curve, and the dotted lines show its 95% confidence interval.